

Fabrication of conducting polymer/noble metal composite nanorings and their enhanced catalytic properties

Supporting information

Liu Yang, Zhen Zhang, Guangdi Nie, Ce Wang, and Xiaofeng Lu*

Alan G. MacDiarmid Institute, College of Chemistry, Jilin University, Changchun
130012, P. R. China

Contents

I. Materials and apparatus	S2
II. Preparation of PPy/Pd nanorings	S2
III. Catalytic reduction of <i>p</i> -nitrophenol by PPy/Pd nanorings	S3
IV. TEM image of PPy/Pd composites and FTIR spectra of PPy/Pd composite nanorings and pure PPy.....	S3
V. Raman spectrum of PPy/Pd composite nanorings	S4
VI. X-ray photoelectron spectroscopy (XPS) measurements of PPy/Pd composite nanorings	S4
VII. UV-vis spectrum of (CTA) ₂ PdBr ₄ complex	S5
VIII. Current–voltage (I–V) characteristics of PPy/Pd composite nanorings	S6
IX. Catalytic activity of PPy/Pd composite nanorings	S7
X. Synthesis of PEDOT/Pd composite nanorings	S8
XI. Characterization of PEDOT/Pd composite nanorings.....	S9

I. Materials and apparatus

3,4-ethylenedioxythiophene monomer was purchased from Beili Pharm Raw Material (Suzhou) Co., Ltd. and used without further purification. Pyrrole monomer was distilled under reduced pressure before use. Pd/C and Pd black were purchased from E-TEK and Sigma-Aldrich, respectively. All the other chemicals were of analytical grade and used as received without further purification.

The morphology of the samples were observed by a cold field-emission scanning electron microscopy (FESEM, Hitachi SU8020) and a transmission electron microscopy (TEM, JEOL JEM-1200 EX) operated at 3.0 and 100 kV, respectively. High-resolution TEM (HRTEM) images and energy dispersive X-ray (EDX) analysis were conducted on a FEI Tecnai G2 F20 electron microscope at an acceleration voltage of 200 kV. FT-IR spectra were recorded on a BRUKER VECTOR22 spectrometer using KBr pellets. Raman spectrum was obtained with a LabRam Aramis Raman spectrometer with a HeNe laser as the excitation line of 633 nm. XRD patterns were obtained with a Siemens D5005 diffractometer using Cu K α radiation. Analysis of the X-ray photoelectron spectra (XPS) was performed on an ESCLAB MKII instrument. The ultraviolet-visible (UV-vis) absorption spectroscopy was performed on SHIMADZU UV-2501 UV-vis spectrophotometer. The weight percent of Pd in the nanocomposites was determined using an inductive coupled plasma emission spectrometer (ICP, PerkinElmer OPTIMA 3300DV). The current-voltage (I-V) characteristics of PPy/Pd composite nanorings were tested on Keithley Instruments Inc. 2400-C SourceMeter.

II. Preparation of PPy/Pd nanorings

In a typical procedure, 0.15 mmol of CTAB was dissolved in 15 mL of distilled water to form a homogeneous solution. Under stirring, 0.119 mmol of Na₂PdCl₄ in 1 mL of distilled water was added into the above surfactant aqueous solution slowly, resulting in an orange precipitate of (CTA)₂PdBr₄ complex that functions as an oxidative template. The mixture was stirred for 5-10 min, and then heated to 90° C. After another 5 min, 15 μ L of pyrrole monomer was added to the

above mixture and the mixture gradually turned black in color. The reaction mixture was stirred for further 12 h at 90 °C. The resulting black precipitate was centrifuged and then washed several times with water and ethanol, and the solid sample could be obtained by drying at room temperature or freeze-drying.

III. Catalytic reduction of *p*-nitrophenol by PPy/Pd nanorings

Typically, 30 μL of *p*-nitrophenol (7.4 mM) and 30 μL of NaBH_4 (0.41 M) were added into a quartz cuvette containing 2 mL water. Then, 10 μL of an aqueous solution containing PPy/Pd composite nanorings (2.64 mg/mL) was injected into the cuvette to start the reaction. The intensity of the absorption peak at 400 nm in UV-vis spectroscopy was used to monitor the process of the conversion of *p*-nitrophenol to *p*-aminophenol. The catalytic reduction reactions of *p*-nitrophenol were conducted at room temperature.

IV. TEM image of PPy/Pd composites and FTIR spectra of PPy/Pd composite nanorings and pure PPy

PPy/Pd composites synthesized in the absence of CTAB show the granular morphology in Figure S1A. The FT-IR spectra of PPy/Pd nanorings and pure PPy synthesized in the presence of CTAB using $(\text{NH}_4)_2\text{S}_2\text{O}_8$ as oxidant are presented in Figure S1B, indicating that characteristic peaks of PPy/Pd nanorings are almost identical to the pure PPy.

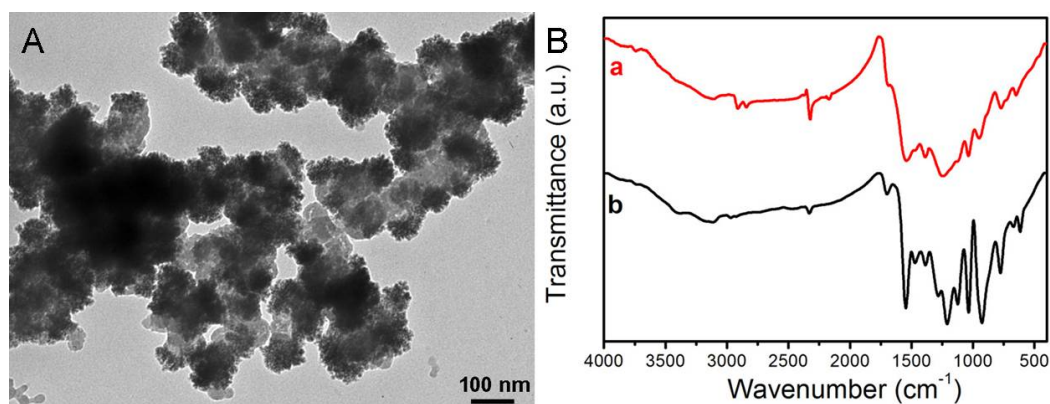


Figure S1(A) TEM image of PPy/Pd composites synthesized in the absence of CTAB; (B) FTIR spectra of (a) PPy/Pd composite nanorings and (b) pure PPy synthesized in the presence of CTAB.

V. Raman spectrum of PPy/Pd composite nanorings

The Raman spectrum is presented in Figure S2, the strong characteristic peaks at around 1562 and 1349 cm^{-1} represent the backbone stretching mode of C=C bond and antisymmetrical C-N stretching of PPy, respectively. The weak band at around 1060 cm^{-1} might be attributed to the N-H in-plane deformation of the oxidized PPy. This result indicated the formation of PPy in the composite nanorings.

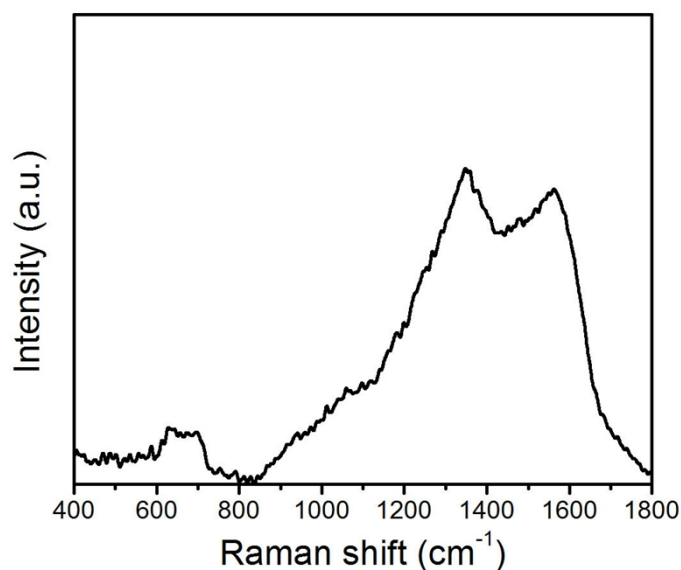


Figure S2 Raman spectrum of PPy/Pd composite nanorings.

VI. X-ray photoelectron spectroscopy (XPS) measurements of PPy/Pd composite nanorings

The surface analysis of XPS of PPy/Pd composite nanorings was used to prove the existence of Pd and PPy in the resulting sample. It is found that the characteristic signals for Pd, C and N are clearly detected in the as-prepared PPy/Pd composite nanorings. The Pd3d peaks could be deconvoluted into two doublet components in the spectrum, which are centered at 335.6, 337.9, 340.9, 343.2 eV. The low binding energy signals at 335.6 eV(Pd3d_{5/2}) and 340.9 eV(Pd3d_{3/2}) are assigned to Pd(0), while another two peaks at 337.9 eV (Pd3d_{5/2}) and 343.2 eV (Pd3d_{3/2}) are related to oxidized Pd(II) salts.

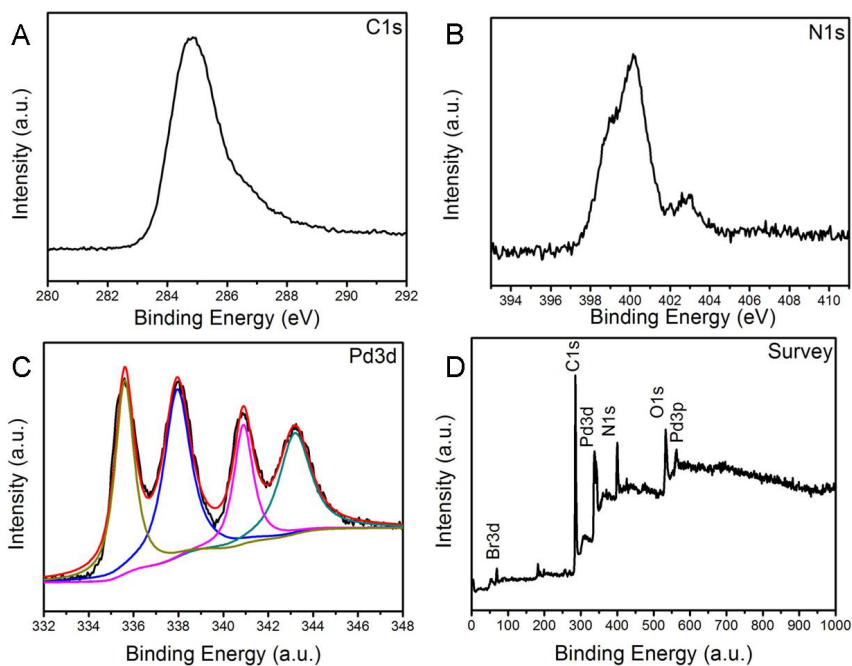


Figure S3 XPS spectra of PPy/Pd composite nanorings (A) C1s, (B) N1s, (C) Pd3d and (D) full survey spectrum.

VII. UV-vis spectrum of $(CTA)_2PdBr_4$ complex

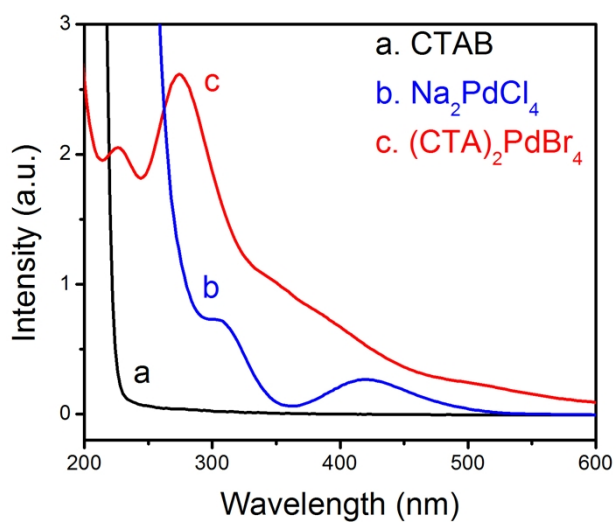


Figure S4 UV-vis spectra of (a) CTAB, (b) Na_2PdCl_4 and (c) Na_2PdCl_4 solution after the addition of CTAB.

VIII. Current–voltage (I–V) characteristics of PPy/Pd composite nanorings

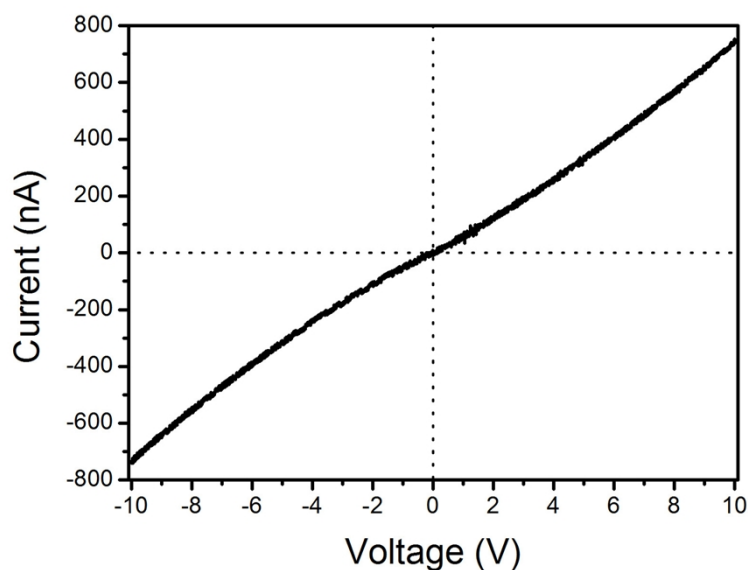


Figure S5 Current–voltage (I–V) characteristics of PPy/Pd composite nanorings.

The dried samples were re-dispersed into water and dropped onto the surface of an interdigital electrode. The dried interdigital electrode was used to test the current(I)–voltage(V) characteristics of PPy/Pd composite nanorings on 2400-C SourceMeter from +10 to –10 V. As shown in Figure S4, it is observed from the figure that at room temperature the current varies non-linearly but is symmetric with respect to the polarity of the applied voltage range of +10 to –10 V. The results suggest that the electron conduction across the PPy/Pd composite nanorings is inhomogeneous, with localized regions of high conductivity. This non-linear I–V behavior can be attributed to the tunneling and hopping contributions to transport across the barriers.

IX. Catalytic activity of PPy/Pd composite nanorings

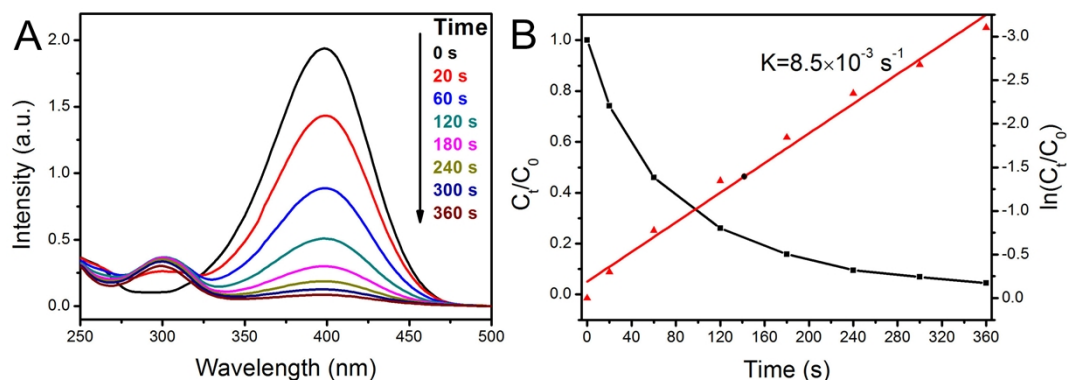


Figure S6 UV-Vis absorption spectra for the catalytic reduction of *p*-nitrophenol by NaBH_4 over PPy/Pd composite nanorings; The squares and triangles stand for the C_t/C_0 and $\ln(C_t/C_0)$ versus reaction time for the reduction of *p*-nitrophenol by NaBH_4 over PPy/Pd composite nanorings. C_0 stands for the intensity of the absorption at 400 nm initially and C_t was the absorption peak at time t .

We evaluated the catalytic activity of the PPy/Pd composite nanorings by catalyzing the reduction of *p*-nitrophenol into *p*-aminophenol by NaBH_4 in aqueous solution. The intensity of the absorption peak at 400 nm in UV-vis spectroscopy was used to monitor the process of the conversion of *p*-nitrophenol to *p*-aminophenol. From Figure S6, the peak at about 400 nm almost disappeared after 6 min, indicating that the reduction of *p*-nitrophenol into *p*-aminophenol by NaBH_4 was almost complete. The kinetic apparent rate constant for the reduction of *p*-nitrophenol by using the PPy/Pd composite nanorings was calculated to be about $8.5 \times 10^{-3} \text{ s}^{-1}$ (Figure S6B).

For comparison, the catalytic activities of commercial Pd/C, PPy/Pd composites synthesized in the absence of CTAB and commercial Pd black were also tested in the same condition. The kinetic apparent rate constants were shown in Figure S7.

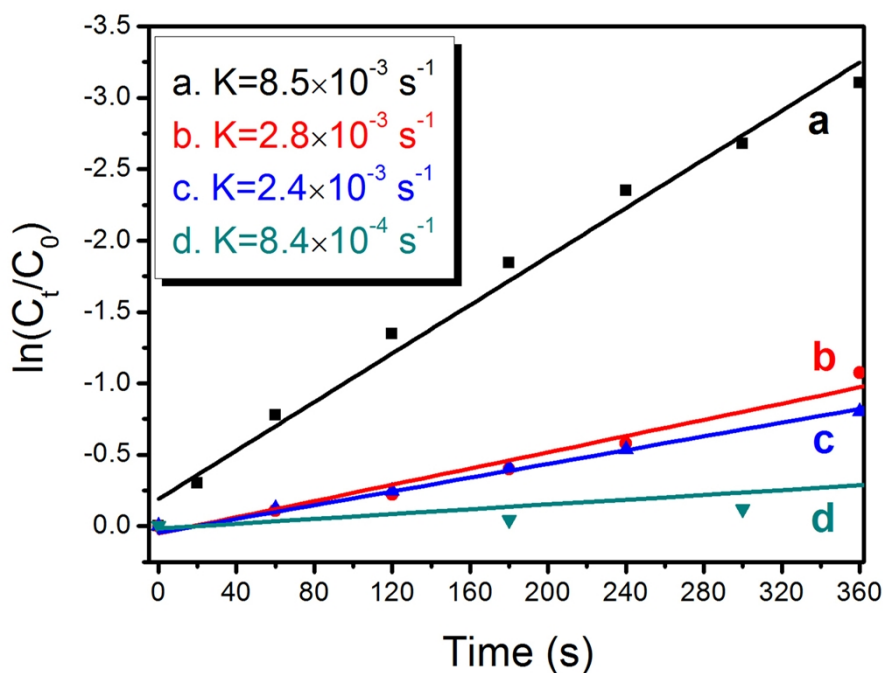


Figure S7 $\ln(C_t/C_0)$ versus reaction time for the reduction of *p*-nitrophenol by NaBH_4 over (A) PPy/Pd composite nanorings (B) commercial Pd/C (C) PPy/Pd composites and (D) commercial Pd black. C_0 stands for the intensity of the absorption at 400 nm initially and C_t was the absorption peak at time t . The kinetic apparent rate constants were calculated to be about $8.5 \times 10^{-3} \text{ s}^{-1}$, $2.8 \times 10^{-3} \text{ s}^{-1}$, $2.4 \times 10^{-3} \text{ s}^{-1}$ and $8.4 \times 10^{-4} \text{ s}^{-1}$, respectively.

X. Synthesis of PEDOT/Pd composite nanorings

In a typical synthesis of PEDOT/Pd composite nanorings, 0.15 mmol CTAB was dissolved in 15 mL distilled water to form a homogeneous solution. Under stirring, 0.119 mmol sodium Na_2PdCl_4 in 1 mL distilled water was added to the above surfactant aqueous solution slowly, resulting in an orange precipitate of $(\text{CTA})_2\text{PdBr}_4$ complex that functions as an oxidative template. The mixture was stirred for 5-10 min, and the heated to 90°C . After another 5 min, 15 μL 3,4-ethylenedioxythiophene (EDOT) monomer was then added to the above mixture and the mixture gradually turned black in color. The reaction mixture was stirred for 12 h at 90°C . The resulting black precipitate was washed several times with water and methanol, and then dried at room temperature.

XI. Characterization of PEDOT/Pd composite nanorings

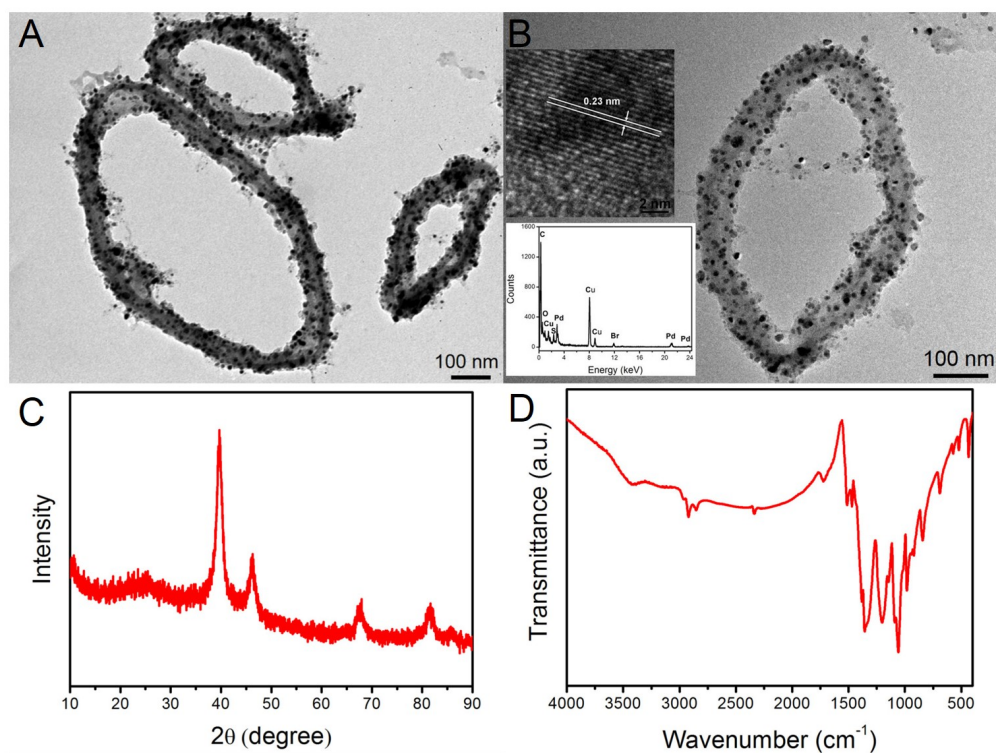


Figure S8 (A) TEM image, (B) HRTEM images, (C) XRD pattern and (D) FT-IR spectrum of PEDOT/Pd composite nanorings.

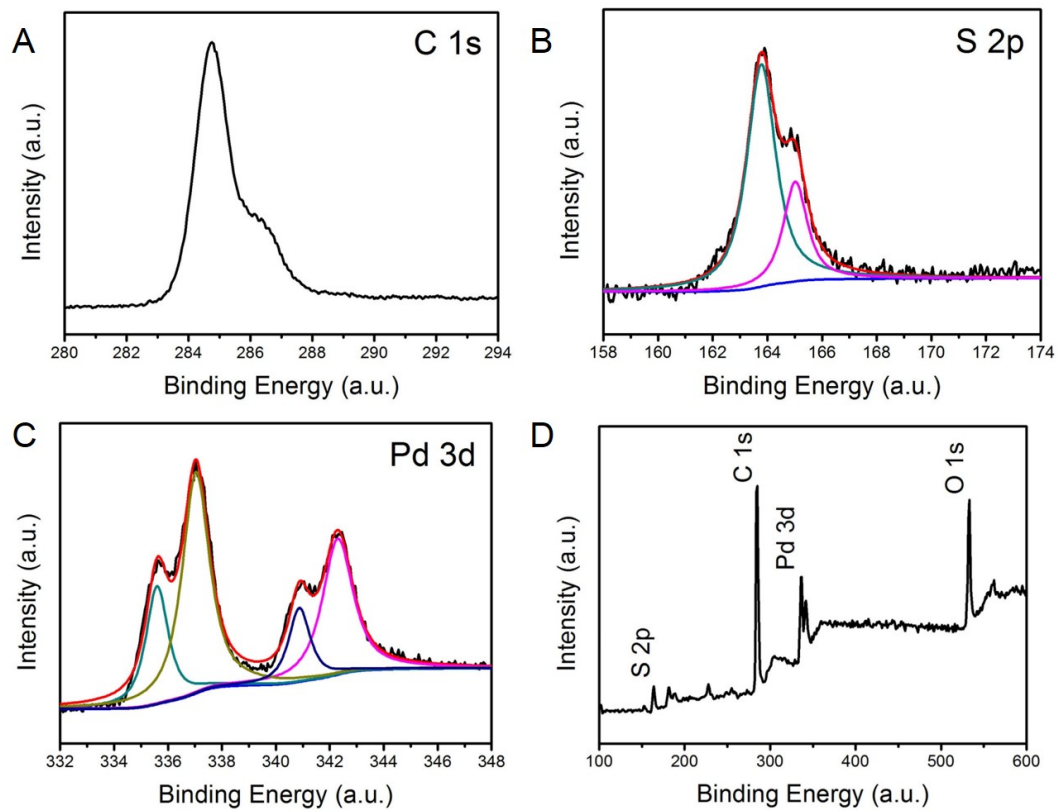


Figure S9 XPS spectra of PEDOT/Pd composite nanorings (A) C1s, (B) S2p, (C) Pd3d and (D) full survey spectrum.